2009 ASME International Mechanical Engineering Congress & Exposition
IMECE2009
November 13-19, 2009, Lake Buena Vista, Florida, USA

IMECE2009-12784

FINITE ELEMENT ANALYSIS OF A LOCKED BOLT WITH AN INITIAL CRACK

Jean Paul Kabche
Engineering Simulation and Scientific Software
Rio de Janeiro, RJ, Brazil

Maurício Rangel Pacheco
Engineering Simulation and Scientific Software
Rio de Janeiro, RJ, Brazil

Ivan Thesi
Engineering Simulation and Scientific Software
Rio de Janeiro, RJ, Brazil

Luiz Carlos Largura
PETROBRAS
Rio de Janeiro, RJ, Brazil

ABSTRACT

Bolted connections are largely employed in various types of engineering structures to transfer loads from one member to another. In particular, the off-shore industry has made extensive use of these connections, predominantly at the sub-sea level. In spite of their advantages, bolted joints are critical regions and may become sources of structural weakness due to large stress concentrations. Under severe operating conditions, micro-cracks can develop in the bolt, creating regions of elevated stress which may significantly reduce the integrity of the connection and ultimately lead to failure. This paper presents the three-dimensional finite element analysis of a steel locked bolt assembly aimed to assess the effect of micro-cracks on the structural integrity of the assembly using the commercial finite element package ANSYS. Non-linear contact between the bolt and nut threads is considered, where frictional sliding between components is allowed. A bi-linear isotropic hardening model is used to account for non-linear material behavior. The assembly is loaded by applying a pre-load of fifty percent of the yield stress of the material, according to the API-6A Norm. Two geometric models are investigated: a healthy locked bolt assembly with no initial cracks; and a damaged model, where a circular crack is introduced at the root of the bolt threads. The effect of the crack size is studied by modeling the crack with three different radius sizes. The J-Integral fracture mechanics methodology was used to study the stress concentrations in the damaged model.

INTRODUCTION

Bolted connections have been used in many engineering applications to transfer loads between components. In spite of their ease of use and assembly, bolted joints are critical regions and may become sources of structural weakness due to large stress concentrations. Furthermore, at severe operating conditions, micro-cracks can develop in the bolt, thus creating regions of high stresses which may significantly reduce the integrity of the connection and ultimately lead to failure. Finite element analysis has become a feasible alternative to study the onset of damage and investigate the effect of cracks on the mechanical behavior of joints and bolt members used in these joints.

Use of numerical simulations can significantly reduce the need for costly laboratory testing and it is an area where much research has been conducted. For example, Toribio [1] studied surface cracks in the thread ground of bolts subjected to axial loading directly applied by the nut using the finite element method with quarter-point singular isoparametric elements along the crack front. The stress intensity factor was calculated through the stiffness derivative method, by using a virtual crack extension technique to compute the energy release rate. This study found that direct loading on the thread flank by a nut increases the stress intensity factor. Further, this effect decreased with the crack length. For the deepest circular cracks, however, nut loading showed relaxation of the K-value, mainly at the crack surface. Renauld and Lien [2] investigated the evolution of global and local stress/strain conditions in test fasteners under tension using elastic-plastic, time-dependent, finite element analyses (FEA). Fastener models were constructed with automated routines and contact conditions were prescribed at all potential mating surfaces. Thermal or mechanical pre-loading was followed by a temperature ramp and a dwell time at constant temperature. Their study showed that while the amount of thermal stress relaxation was limited for the conditions modeled, local stress states were highly dependent upon geometry, pre-loading history, and thermal expansion differences between the test fastener and test fixture. Atre and Johnson [3] applied a finite element methodology to a quasi-static, displacement controlled riveting process to capture the residual stresses in riveted lap joints. Their three-

dimensional finite element model considered material, geometric, and contact non-linearities to simulate the joining process. Upon conducting geometric parametric studies, it was found that the tensile hoop stress was the primary source of fatigue cracks in the joints. Additionally, they developed a relationship between the rivet-head deformation ratio and the rivet-head height with applied displacement as a means of controlling the rivet-head deformation. Olsen [4] performed crack growth analyses on roll-threaded fasteners under tensile fatigue conditions. He presented a comparison of five leading methods to determine the stress intensity multiplication factor, $Y(a/d)$, for threaded fasteners, based on experimental data, analytic equations, FE methods, or a combination thereof. By comparing and considering these five methods together, critical observations were made to guide future research based on these state-of-practice solution methods. Milan et. al. [5] used tensile, impact and hardness testing to fully characterize the component and material properties of SAE 4340 steel locking bolts used to assemble speed reducer housings which fractured after a few hours of operation. Then, stress calculations were performed using both Neuber analysis and finite element analysis and the results were compared. Their study found that cracks in the bolt nucleated at the root of the last engaged thread due to a combination of high local stresses in this region, surface defects, non-uniformity of the thread root, and low toughness of the material. After nucleation, the crack propagated by fatigue until catastrophic failure took place.

FINITE ELEMENT MODEL WITH NO INITIAL CRACK

3D Geometry

The single stud bolt and nut assembly configuration considered for this study is shown in Figure 1. It is noted that the bolt threads are included in the geometry to accurately represent the local stresses developed between the bolt and the nut once a bolt preload is applied. An 8-thread series (8-UN/8 - UNR) bolt, with a nominal diameter of 47.63 mm, is used. Its thread dimensions, according to ASME B1.1 [6], are summarized in Table 1.

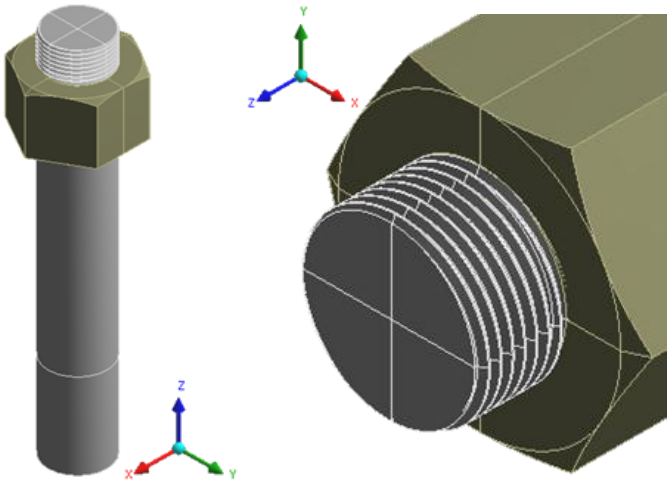

Figure 1 – Solid model of the 3D bolt geometry

Table 1 – Basic thread dimensions of a 47.63-mm bolt, according to ASME B1.1

Parameter	Description	Value
D	Basic major diameter	47.625 mm
D_2	Basic pitch diameter	45.563 mm
d_3	Design minor diameter, external	43.845 mm
D_1	Design minor diameter, internal	44.188 mm
λ	Lead angle at basic pitch dia.	1 deg
A_d	Section at minor diameter	1483 mm^2
A_s	Tensile stress area	1555 mm^2

Material Properties

The bolt and nut are both modeled using material properties for AISI 4340, which is a heat-treatable, low alloy steel. AISI 4340 is known for its toughness and capability to develop high strength in the heat treated condition while retaining good fatigue strength. To account for material behavior beyond the linear-elastic range, elastic-plastic material properties are used, as summarized in Table 2.

Table 2 – Material properties for AISI 4340

Property	Description	Value
E	Modulus of elasticity	205 GPa
σ_y	Yield stress	1141.05 MPa
σ_u	Ultimate stress	1304.21 MPa
ε_y	Yield strain	0.0018 mm/mm
ε_u	Ultimate strain	0.0594 mm/mm
H	Elastic-plastic tangent modulus	2832.62 MPa

Finite Element Mesh

The finite element mesh of the bolt and nut is built using three-dimensional solid elements SOLID186 and SOLID187. SOLID186 is a second order, 20-node solid element with quadratic displacement behavior; SOLID187 is a second order, 10-node solid element with quadratic displacement behavior, and is well suited to model irregular meshes, such as in the bolt thread regions. Both element types have three degrees of freedom at each node: translations in the nodal x, y, and z directions. The mesh consists of 219207 elements and 360653 nodes. Figure 2a shows the complete meshed model. Figures 2b and 2c show the bolt thread details, where it is observed that a much finer mesh is used in this region in order to accurately capture the high stress gradients.

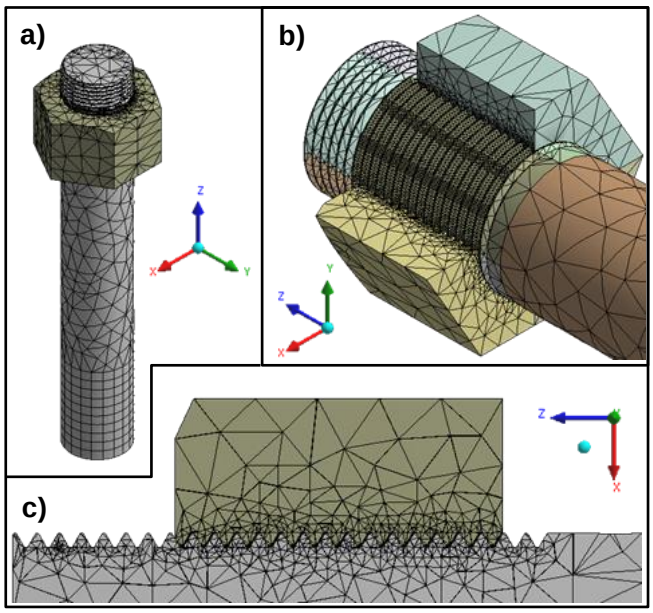

Figure 2 – Meshed finite element model. a) Complete model. b) Cut-view showing bolt threads detail. c) Side view of contact regions between bolt and nut threads.

Loading and Boundary Conditions

Figure 3 shows the boundary conditions applied to the finite element model. A fixed boundary condition (i.e. all displacements are equal to zero) was applied at the lower section of the bolt. To simulate compression of the lower surface of the nut, a simple support was defined (i.e. U_x = free, U_y = free, U_z = 0), thereby allowing lateral expansion of the nut. Bolt pre-tension was defined by applying a load of 761 kN to the mid-surface of region "C" (region in red), which is about fifty percent of the yield stress of the material, according to the API-6A Norm [7]. Pre-tension load was computed based on a torque T = 6102 kN·mm and following the recommendations in ASME B1.1 [6].

Frictional contact behavior was defined between the bolt threads and the nut to account for their mechanical interaction. A static friction coefficient of 0.13 was used, as recommended in ASME B1.1. The Augmented Lagrange formulation was used to alleviate contact interaction issues related to contact penetration and solution convergence.

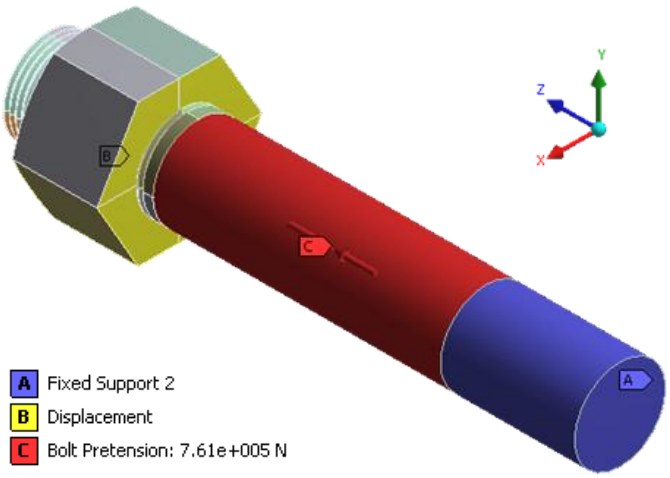

Figure 3 – Boundary conditions applied to FE model

FINITE ELEMENT MODEL WITH AN INITIAL CRACK

The geometry of the stud bolt and the nut is the same as that used for the previous analysis, except that a crack region which is explicitly introduced into the new geometry. To model a crack in the bolt, a technique called sub-modeling was employed. The rationale for using this method is that the original mesh used in Figure 2 may not be appropriate to accurately capture the high stress gradients present at the crack location. Additionally, it may be computationally unfeasible to reanalyze the entire model using a greater mesh refinement in order to obtain more accurate results. Sub-modeling allows the analyst to generate an independent and more refined meshed model of only the region of interest (sub-model) and then analyze it, thus maintaining a reasonable computational effort.

Sub-modeling uses a cut-boundary interpolation approach. A cut boundary is the boundary of the sub-model which represents a cut through the coarse (original) model. Displacements calculated on the cut boundary of the coarse model are then specified as boundary conditions for the sub-model, thus applying deformation state that the coarse structure experiences. Nodes along the cut boundaries are identified, and ANSYS calculates the DOF values (displacements) at those nodes by interpolating results from the full (coarse) model. This step was achieved by using a script created with APDL (ANSYS Parametric Design Language).

Circular cracks were explicitly created as part of the geometry of the threaded bolt in ANSYS Workbench Design Modeler. Three different crack sizes were used: one quarter of the nominal radius (*R/4*), half of the nominal radius (*R/2*), and one bolt radius (*R*), as shown in Figure 4.

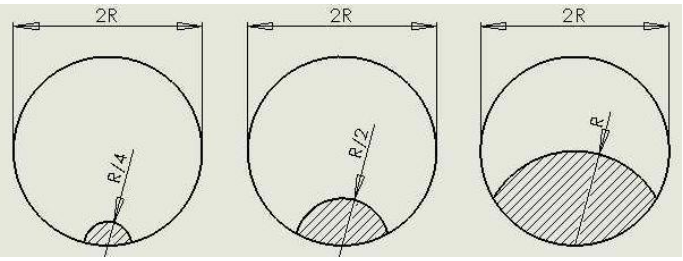

Figure 4 – Size of the cracks used in the finite element sub-models

A comparison of the full meshed model versus the sub-model is shown in Figure 5. To study the influence of the crack size on the bolt stresses, the sub-model built only consists of about half of the nut volume and nine threads. As shown in Figure 6, significant mesh refinement is clearly observed, with a total sub-model mesh of 321,279 elements and 491,160 nodes.

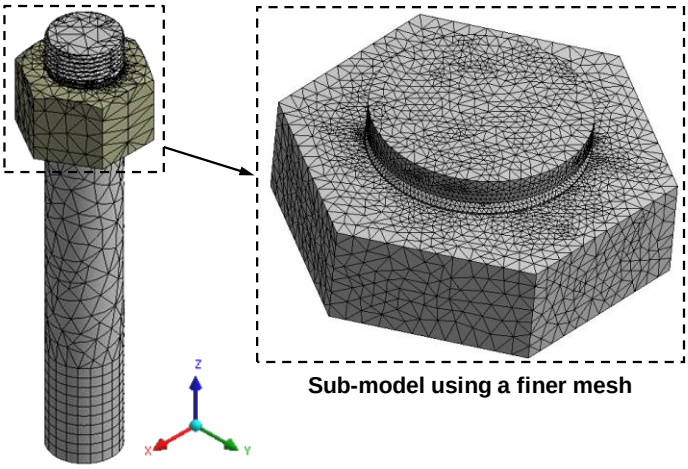

Figure 5 – Full meshed model versus sub-model

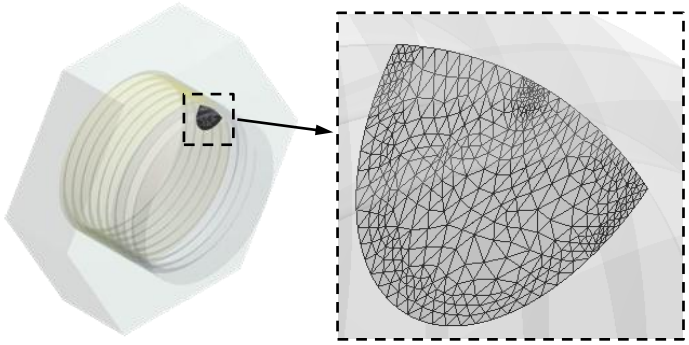

a) Coincident with one quarter of the bolt nominal diameter, *R/4*

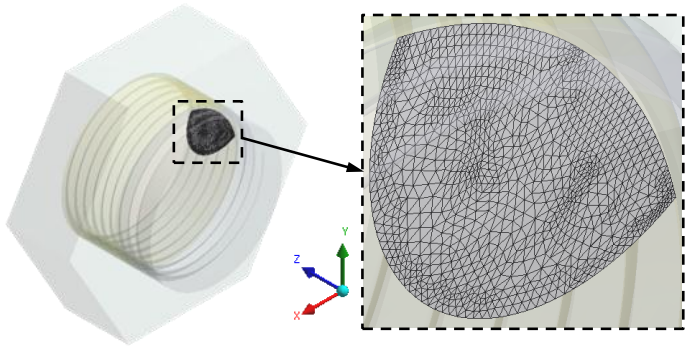

b) Coincident with half of the bolt nominal diameter, *R/2*

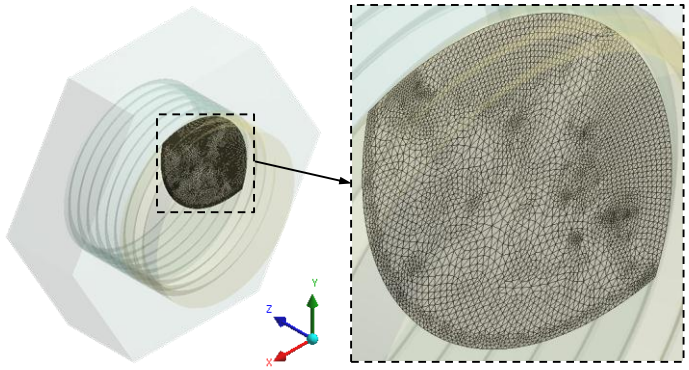

c) Coincident with the bolt nominal diameter, *R*

Figure 6 – Crack mesh detail for various sizes

RESULTS

Bolt model with no initial crack

The model with no initial crack was used to determine the stress state in a healthy stud bolt and to verify that the correct mechanical behavior was being modeled. A peak plastic strain of 0.01747 mm/mm (stud bolt) was computed near the bottom region of the nut, well into the plastic region of the material response, as shown in Figure 7. A peak plastic strain of 0.02963 mm/mm was observed in the nut. These values correspond to thread regions of peak frictional contact with the

nut. A contour plot for the maximum principal stresses in the stud bolt is presented in Figure 8, which again shows that the lower bolt threads near the end of the nut region experience a peak tensile stress of about 2060 MPa, while the peak stress in the nut is about 1227 MPa. These results are summarized in Table 3.

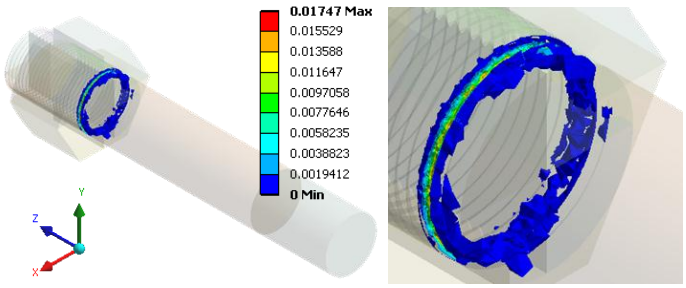

Figure 7 – Equivalent plastic strain in the bolt (mm/mm)

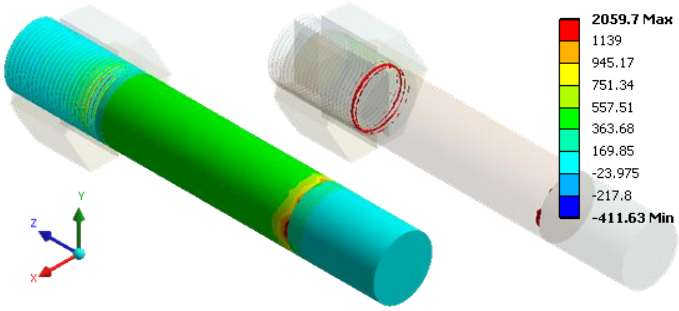

Figure 8 – Maximum principal stress in the bolt (MPa)

Table 3 – Results of bolt model with no initial crack

Region	von Mises stress (MPa)	Maximum principal stress (MPa)	Equivalent plastic strain (mm/mm)
Stud bolt	1377.50	2059.70	0.01747
Nut	1356.00	1227.30	0.02963

Bolt model with an initial crack

The inclusion of a geometric crack into the finite element model results in increased local stresses around the crack region, as expected. For the case of a crack size equal to the nominal bolt radius, *R*, Figure 9 shows that the peak maximum principal stress occur in the stud bolt, with a magnitude of 2119 MPa. The maximum principal stresses in the crack are shown in Figure 10, with a peak tensile magnitude of 2099 MPa. Results for crack sizes of one quarter and one half of the bolt nominal diameter are presented in Table 4.

To observe the effect of the crack on the stress along the crack surface, maximum stress values were recorded at various locations along a bolt cross-section in the x-y plane, as shown in Figure 11. This figure shows that for areas away from the crack, the maximum principal stress in the bolt is highest, and it decreases as the crack region is approached, with a total variation of about 132 MPa from end to end, along the centerline of the bolt cross-section. This is explained by the fact that the material near the crack has become fully plastic and the stresses in this area are subsequently transferred to the rest of the section.

Further, a J-Integral calculation was performed to compute the strain energy release rate, or energy per unit fracture surface area in the material. Thus, it is possible to characterize fracture under elastic-plastic and fully plastic conditions. As expected, Figure 12 shows that the energy release rate peaks at the ends of the crack tip.

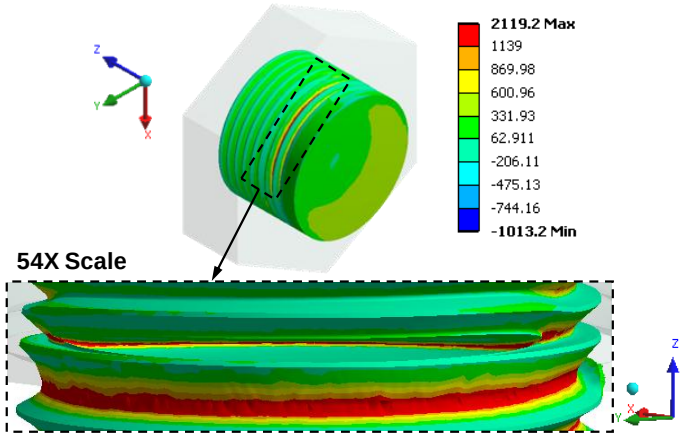

Figure 9 – Maximum principal stress in the bolt using a crack size of *R* (MPa)

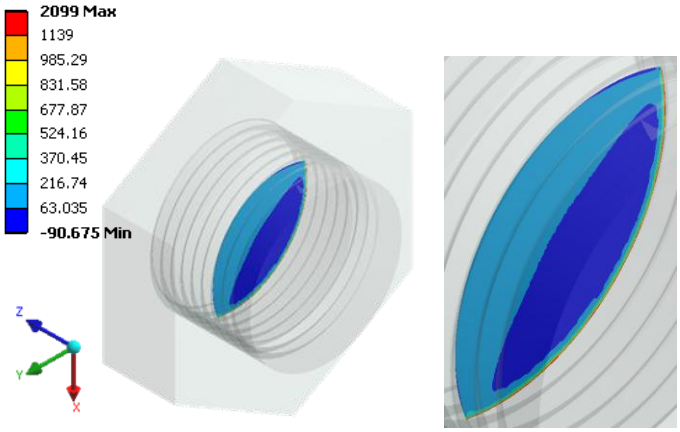

Figure 10 – Maximum principal stress in the crack using a crack size of *R* (MPa)

Table 4 – Results of model with an initial crack

Crack size	von Mises Stress (MPa)	Maximum principal stress (MPa)	Equivalent plastic strain (mm/mm)
R/4	1307.90	1939.70	0.04559
R/2	1259	1801.90	0.06224
R	1412.40	2099	0.01747

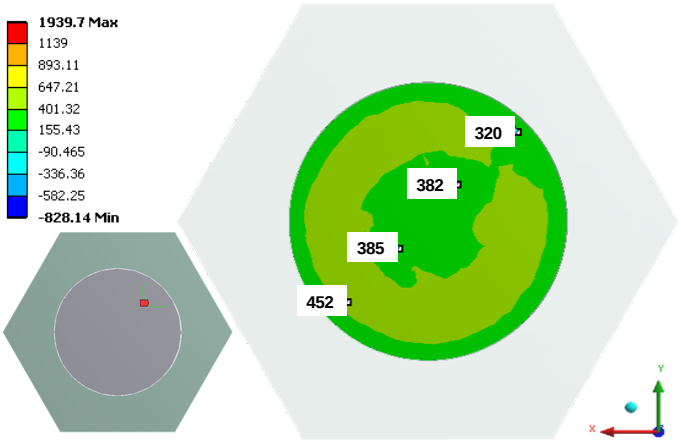

Figure 11 – Maximum principal stress variation in the bolt along crack surface using a crack size of *R* (MPa)

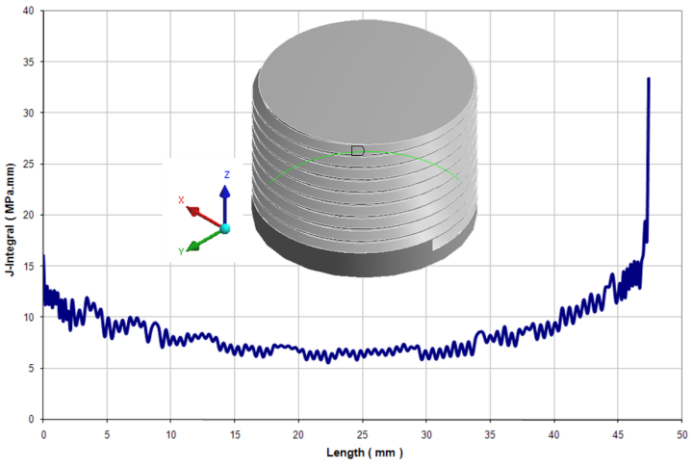

Figure 12 – J-Integral using a crack size of *R*

SUMMARY

This paper presents the three-dimensional finite element analysis of a steel locked bolt assembly using the commercial finite element package ANSYS. Non-linear contact between the bolt and nut threads was included, by allowing frictional sliding between the nut and bolt. A bi-linear isotropic hardening model was used to account for non-linear material behavior. The assembly was loaded by applying a pre-load of fifty percent of the yield stress of the material, according to the API-6A Norm. Two geometric models are investigated: a healthy assembly with no initial cracks; and a damaged model, where a circular crack is introduced at the root of the bolt threads. Results of the healthy model show that the lower bolt threads near the end of the nut region experience the largest tensile stresses. Results of the damaged model showed that increasing the crack size increases the peak plastic strain, but has a modest effect on the maximum principal stresses. It was also observed that for areas away from the crack, the maximum principal stress in the bolt is highest, and it decreases as the crack region is approached. Lastly, using the J-Integral fracture mechanics approach showed that the energy release rate peaks at the ends of the crack tip.

REFERENCES

[1] Toribio, J. "Stress intensity factor solutions for a cracked bolt loaded by a nut," International Journal of Fracture, 53(4): 367-385, 1992.

[2] Renauld, M.L. and Lien, H. "Probing the elastic-plastic, time-dependent response of test fasteners using finite element analysis (FEA)," Third Symposium on Structural Integrity of Fasteners Including the Effects of Environment and Stress Corrosion Cracking (SCC), American Society for Testing and Materials, West Conshohocken, PA, 2004.

[3] Atre, A and Johnson, W. S. “3D FEA Simulations to Assess Residual Stresses in Riveting Processes,” STP1487: Structural Integrity of Fasteners Including the Effects of Environment and Stress Corrosion Cracking, Vol. 3, 2007.

[4] Olsen, K. W. “Fatigue Crack Growth Analyses of Aerospace Threaded Fasteners - Part I: State-of-Practice Bolt Crack Growth Analyses Methods,” STP1487: Structural Integrity of Fasteners Including the Effects of Environment and Stress Corrosion Cracking, Vol. 3, 2007.

[5] Milan, M. T., Spinelli, D., Bose, W. W., Montezuma, M. F., and Titab, V. “Failure analysis of a SAE 4340 steel locking bolt,” Engineering Failure Analysis, 11(6): 915-924, 2004.

[6] ASME B1.1: 2003 Unified Inch Screw Threads, (UN and UNR Thread Form), ISBN #: 0791828336, 2003.

[7] API 6A: Specification for Wellhead and Christmas Tree Equipment, American Petroleum, 19th Edition, 2009.

[8] Ansys Inc., Structural Analysis Guide, Release 11, 2007.